Available online at www.sciencedirect.com
SCIENCE DIRECT®
Biochemical and Biophysical Research Communications 338 (2005) 355–364
BBRC
www.elsevier.com/locate/ybbrc

Review

Freeze-quenched iron-oxo intermediates in cytochromes P450

Christiane Jung [a,*,1], Volker Schünemann [b], Friedhelm Lendzian [c]

[a] *Max-Delbrück-Center for Molecular Medicine, 13125 Berlin, Germany*
[b] *Technical University of Kaiserslautern, Department of Physics, 67663 Kaiserslautern, Germany*
[c] *Max-Volmer Laboratory for Biophysical Chemistry, Technical University Berlin, PC 14, 10623 Berlin, Germany*

Received 15 August 2005
Available online 29 August 2005

Abstract

Since the discovery of cytochromes P450 and their assignment to heme proteins a reactive iron-oxo intermediate as the hydroxylating species has been discussed. It is believed that the electronic structure of this intermediate corresponds to an iron(IV)–porphyrin-π-cation radical system (Compound I). To trap this intermediate the reaction of P450 with oxidants (shunt pathway) has been used. The common approaches are stopped-flow experiments with UV–visible spectroscopic detection or rapid-mixing/freeze-quench studies with EPR and Mössbauer spectroscopic characterization of the trapped intermediate. Surprisingly, the two approaches seem to give conflicting results. While the stopped-flow data indicate the formation of a porphyrin-π-cation radical, no such species is seen by EPR spectroscopy, although the Mössbauer data indicate iron(IV) for P450cam (CYP101) and P450BMP (CYP102). Instead, radicals on tyrosine and tryptophan residues are observed. These findings are reviewed and discussed with respect to intramolecular electron transfer from aromatic amino acids to a presumably transiently formed porphyrin-π-cation radical.

Keywords: Compound I; Thiolate heme proteins; Radicals; Mössbauer spectroscopy; Multifrequency EPR; Rapid mixing/freeze quench

Oxygen—"the elixir of life," first recognized in the late 16th century by Michael Sendivogius, a Polish alchemist, philosopher, and medical doctor, and about 150 years later again discovered independently by the Swedish pharmacist Carl Wilhelm Scheele and the English theologian, philosopher, and researcher Joseph Priestley—is a fascinating element. In binding with itself to form molecular oxygen it reveals a significant multiface behavior. Fifty years ago it was Osamu Hayaishi who showed for the first time that an enzyme (pyrocatechase) is involved in catalyzing the incorporation of two atoms of molecular oxygen into an organic compound and he termed such enzymes oxygenases [1]. Around that time many in vivo studies on drug/steroid metabolism were performed [2], culminating a few years later in the discovery of the responsible monooxygenase enzyme cytochrome P450 [3,4]. Since these enzymes have been assigned to a heme protein [5,6] the existence of a highly reactive iron-oxo intermediate is discussed. It is amazing how this discussion has continued and even increased over the past 50 years. The reason is probably that this species is so short-lived and therefore very difficult to analyze. Attempts to trap this intermediate resulted in controversial findings. Suggestions about the chemical and electronic structure came from metal porphyrin studies and from the peroxidase field [7,8], where this intermediate is called Compound I (cpd I). In particular, the analogy to chloroperoxidase from *Caldariomyces fumago* (CPO) suggested that cpd I in P450 should be characterized by an iron(IV) and a porphyrin-π-cation radical.

Seven years ago we entered into the field with the vision of proving this suggestion by a rapid-mixing/freeze-quench technique and of characterizing the putative cpd I of P450cam by EPR and Mössbauer spectroscopy. To our surprise, these studies revealed that instead of the porphy-

* Corresponding author. Fax: +41 41 8104508.
E-mail address: christiane_jung@hotmail.com (C. Jung).
[1] Present address: KKS Ultraschall AG, Frauholzring 29, CH-6422 Steinen, Switzerland.

0006-291X/$ - see front matter © 2005 Elsevier Inc. All rights reserved.
doi:10.1016/j.bbrc.2005.08.166

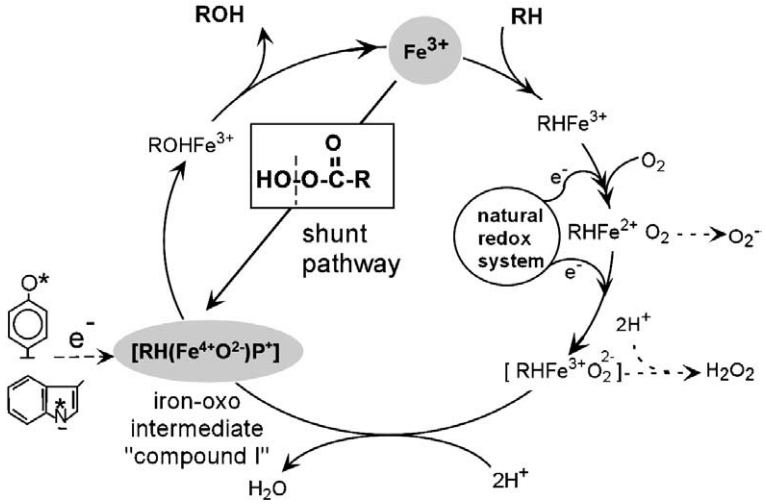

Fig. 1. The heme-based reaction cycle for cytochrome P450, indicating the shunt pathway and the iron-oxo intermediate that is involved in the tyrosine and tryptophan radical formation as side reaction. The uncoupling H_2O_2 and O_2^- reactions are also indicated.

rin radical, a tyrosine radical was formed, although iron(IV) is seen when this species is produced in the reaction of ferric P450cam with external oxidants within the so-called shunt pathway [9] (Fig. 1). In the present paper, we review the main results of these studies on cytochromes P450 and make the comparison to CPO and nitric oxide synthase (NOS) which both form together with P450 the class of thiolate heme proteins. It will be shown that in the light of analogous studies on many other heme proteins performed by several laboratories in the recent years the existence of intermediate protein radicals in P450 is not as surprising as originally thought and might be a general phenomenon in heme-based oxygenases.

The cytochrome P450 reaction cycle

The reaction cycle of P450 (Fig. 1) [10] starts with binding the substrate to the heme protein. The next step is the reduction of the heme iron by electron transfer from NAD(P)H via the redox proteins (flavin protein, iron–sulfur protein). In a subsequent step the reduced heme iron binds molecular oxygen. The dioxygen complex accepts a second electron with synchronous or subsequent attachment of a proton to the oxygen ligand. This intermediate dioxygen species quickly decomposes by splitting the O—O bond and by releasing a water molecule. Thus a highly reactive iron-oxo species (cpd I) is formed, which is assumed to hydroxylate the substrate. This iron-oxo intermediate can also be produced by reaction of the heme enzyme with external oxidants such as peracids, peroxides, and iodosobenzene (shunt pathway), for which substrate conversion was been observed already in the early 70th [11]. This strongly suggests that the intermediate formed with external oxidants may be identical with that formed in the natural reaction cycle via the dioxygen complex and may justify producing cpd I by the shunt pathway for further characterization.

Chloroperoxidase as reference protein

So far, there are two main approaches to identifying the intermediate: (i) the stopped-flow technique taking the heme UV–visible spectrum for detection and (ii) the rapid-mixing/freeze-quench technique using EPR and Mössbauer spectroscopy for characterization of the trapped intermediate. For both approaches CPO is taken as a reference. When CPO is mixed in stopped-flow experiments with an oxidant such as H_2O_2, peroxyacetic acid (PA), or *meta*-chloroperbenzoic acid (mCPBA), a green-colored cpd I is formed, which shows a UV–visible absorption spectrum after several milliseconds, characterized by a broad Soret band around 370 nm and a weak but significant long-wavelength band at ~680 nm [12,13]. This spectrum is characteristic of a porphyrin-π-cation radical, very well known from iron porphyrin model complexes [8]. EPR (9.6-GHz) and Mössbauer spectroscopic studies on CPO samples obtained by rapid-mixing with PA and freeze-quenching [14] identified cpd I as an Fe(IV)=O (spin $S = 1$) and porphyrin-π-cation radical (spin $S' = 1/2$), where both spins couple antiferromagnetically. The EPR spectrum of cpd I in CPO produced with peracids has *g*-values $g_{\|} = 2$ and $g_{\perp} = 1.75$. The Mössbauer study gives an isomer shift of $\delta = 0.14\ \text{mm s}^{-1}$ and a quadrupole splitting of $\Delta E_Q = 1.02\ \text{mm s}^{-1}$. The Fe=O stretch vibration of CPO cpd I lies at $790\ \text{cm}^{-1}$, as determined by resonance Raman spectroscopy [15]. Similar values have been found for porphyrin iron-oxo species [16]. One-electron reduction of cpd I reduces the porphyrin radical but leaves the ferryl state of the Fe(IV)=O moiety unchanged. This species is called Compound II (cpd II). The Fe=O distance of CPO

cpd II has recently been determined by EXAFS studies to be 1.82 Å [17].

Attempts to detect Compound I in P450

Stopped-flow experiments with oxidants similar to those described above for CPO have also been performed on P450cam (CYP101) [18] and on thermostable CYP119 [19] with the shortest times for detection being 6 and 2 ms, respectively, using mCPBA as oxidant. In contrast to CPO, the spectrum of an intermediate was only resolved after treatment of a set of spectra at different time points using the single-value decomposition method. It turned out that one single-value component, representing 2–3% of the spectral change, shows a pattern resembling that observed for CPO cpd I. This result has been taken as a proof that a porphyrin-π-cation radical is also formed in P450. On the other hand, Pederson et al. [20], Wagner et al. [21], and Sligar et al. [22] reported optical spectra of an intermediate in the reaction of P450cam with peroxyacetic acid, also obtained by stopped-flow studies with the same time resolution and at subzero (centigrade) temperatures, that do not match the spectra discussed above, probably because of the missing single-value decomposition analysis. Recently, the kinetics of the formation of an intermediate in the reaction of H_2O_2 as well as mCPBA with substoichiometric oxidant concentrations has been studied also with P450cam in the absence and presence of substrates [23]. For the substrate-free protein the rate for the reaction with H_2O_2 decreases with increasing pH, suggesting that a protonation/deprotonation equilibrium of (presumably) Tyr96 should assist intermediate formation. Replacing this tyrosine by alanine removes the pH effect. Very recently, it has been argued, based on stopped-flow studies with UV–visible detection, that the pH value might significantly affect the kinetics and therefore the steady state concentration of a cpd I species in P450cam. Thus the concentration of the cpd I porphyrin radical species as the important electronic entity under reaction conditions might be very low at low pH [24].

Considering only the results of the stopped-flow experiments one might conclude that P450 behaves like CPO. The puzzle began with the rapid-mixing/freeze-quench experiments that we performed first with P450cam from *Pseudomonas putida* (CYP101) [9] and later on with other thiolate heme proteins [25–27].

Trapping the intermediate of P450cam by rapid-mixing/freeze-quench experiments

Equal volumes of a P450 solution and of an oxidant solution (i.e., PA) are rapidly mixed in a rapid-mixing/freeze-quench apparatus, allowing reaction times from 8 ms up to some seconds. The reaction mixture is quenched by spraying into a cold fluid isopentane bath at $T = -110$ °C, and the frozen material thus obtained is packed at the bottom of an EPR tube and a Mössbauer cup using a packing rod made of Teflon. For this purpose a quartz tube and a Teflon cup for the 9.6-GHz EPR and the Mössbauer studies, respectively, are connected to a funnel which is completely immersed into the isopentane bath. For the preparation of the samples for the 94-GHz EPR instrument we have constructed a specific setup [28] that allowed collecting a few grains of freeze-quenched material in a fragile quartz sample tube.

The results on the bacterial cytochrome P450cam from *P. putida* (CYP101) (P450cam) using this technique were initially very surprising. In contrast to the 9.6-GHz EPR spectrum of the freeze-quenched cpd I of CPO with $g_{\|} = 2$ and $g_{\perp} = 1.75$ (Fig. 2), which is characteristic for a porphyrin-π-cation radical ($S' = 1/2$) that couples antiferromagnetically with the iron(IV) ($S = 1$) [14], a signal at $g \sim 2$ with a slight hyperfine structure of the 9.6-GHz signal has been observed for wild-type P450cam, besides the signals of the heme iron low-spin state of the start material (Fig. 2) [9]. The same signals are observed when mCPBA is used as oxidant [28]. In fact, early freeze-quench studies on P450cam and mCPBA by Wagner and Gunsalus [29]

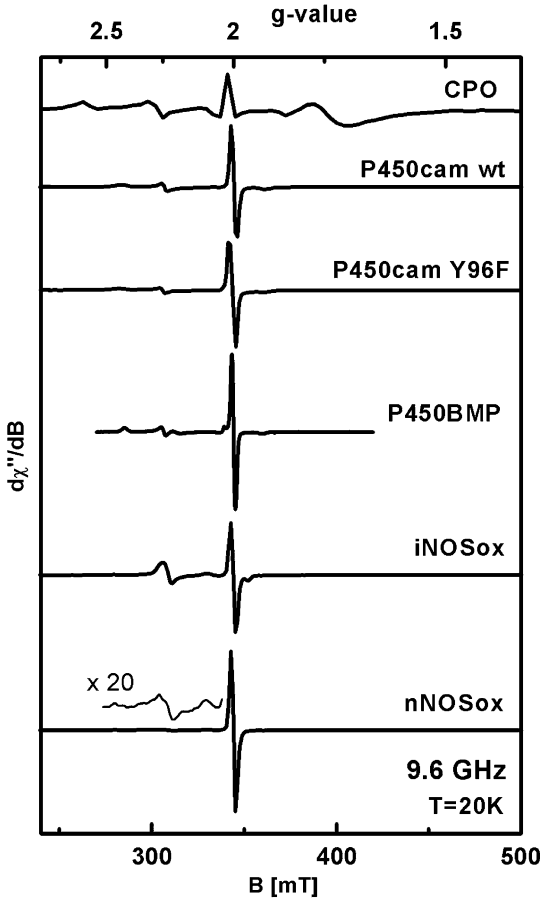

Fig. 2. The 9.6-GHz EPR spectra of CPO, P450cam wild-type, P450cam-Y96F, P450BMP, iNOSox, and nNOSox. All samples were freeze-quenched after 8 ms reaction with peroxy acetic acid. Experimental parameters: $T = 20$ K; microwave power 80 μW; microwave frequency 9.64 GHz; modulation amplitude 0.5 mT; modulation frequency 100 kHz [9,25–28,37].

already revealed a radical EPR signal, which was, however, not further regarded as significant. The saturation behavior of the amplitude of this EPR ($g \sim 2$) signal has a value of $P_{1/2} = 4\ \mu W$ at $T = 4\ K$ (1 mW at 70 K), which is in the range of values observed for tyrosine radicals in proteins [9]. The temperature dependence of the $P_{1/2}$ values indicated enhanced relaxation behavior of the radical spin, suggesting that the site of the radical should be near the paramagnetic heme iron, as would be the case for a radical located, i.e., at Tyr96 in a distance to the iron of about 9.4 Å. Indeed, combined approaches such as high-frequency EPR and site-directed mutagenesis [28] confirmed this initial suggestion.

Assignment of the radical in P450cam by high-frequency EPR spectroscopy and site-directed mutagenesis

Identification and assignment of immobilized amino acid radicals in proteins is by no means easy, because hyperfine and electronic g-value anisotropies lead to significant broadening in the conventional 9.6-GHz EPR spectra. Furthermore, for the case of amino acid radicals, the largest hyperfine splitting results from protons of the side-chain and the hyperfine pattern, observed for the individual protein under consideration, are strongly dependent on the local side-chain geometry. On the other hand, it has been shown that the electronic g-tensor values are independent of these geometrical parameters, and, once they are resolved in the spectra, allow clear discrimination between different types of radicals [30–32]. To unequivocally identify and assign the observed radicals in P450, we have therefore prepared and investigated freeze-quenched samples using 94-, 190-, and 285-GHz EPR [28]. At these frequencies all three g-components were resolved in the spectra. For the radicals in all samples similar g-values were obtained, $g_x = 2.0078$ to 2.0064, $g_y = 2.0044$, and $g_z = 2.0022$, which are fingerprints for tyrosyl radicals [30–33]. The observed distribution of g_x values in all spectra between 2.0078 and 2.0064 indicates a polar environment with heterogeneous hydrogen bonding [33,34].

For a detailed assignment we have used the 94-GHz spectra. Two classes of protons give rise to the observed hyperfine couplings in tyrosine radicals, i.e., the ring protons (α-protons) and the β-protons of the side-chain (Fig. 3). Large couplings arise from the two magnetically equivalent ring protons in the *ortho*-position to the oxygen. Their magnitude depends solely on the π-spin density at the adjacent carbon atom and is very similar for all observed tyrosine radicals. An additional large hyperfine coupling arises from one of the two β-protons of the side-chain. This coupling exhibits only a small anisotropy and its isotropic value, $A_{iso}(H_\beta)$, not only depends on the π-spin density ρ_C^π of the adjacent π-carbon, but is also strongly dependent on the geometry of the side-chain, according to

$$A_{iso}(H_\beta) = \rho_C^\pi (B' + B'' \cos^2\theta), \quad (1)$$

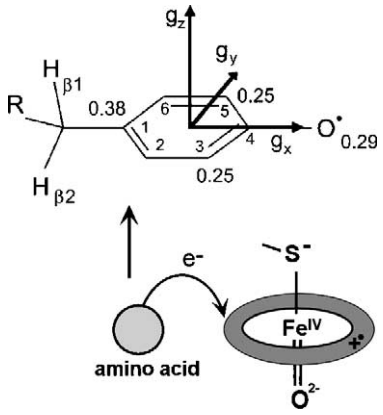

Fig. 3. Molecular structure of the tyrosine radical with atomic numbering (inner numbers) and spin densities (outer numbers) [35]. The indicated g-tensor axis system is collinear with the molecular axis system [63]. The lower sketch indicates the model for the intramolecular electron transfer leading to the amino acid radicals.

where B' and B'' are empirical constants and θ is the dihedral angle between the axis of the π-orbital (p_z) of the adjacent carbon atom and the projected $C_\beta H_\beta$ bond

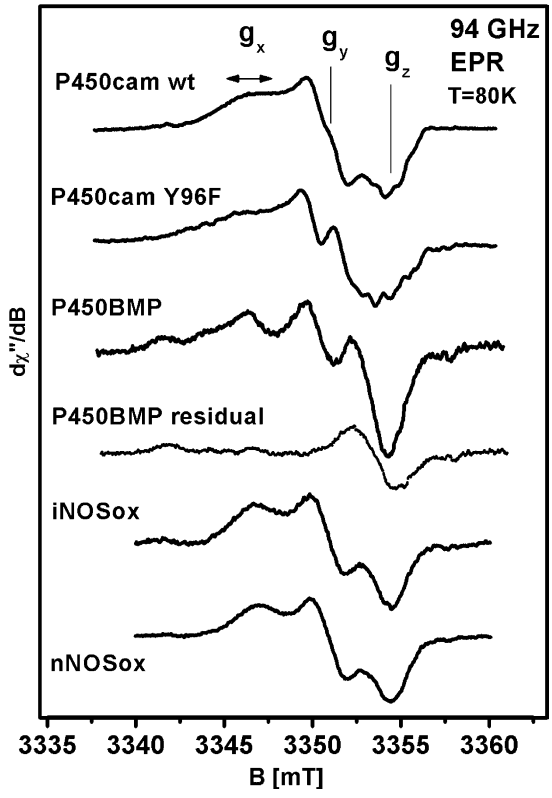

Fig. 4. The 94-GHz EPR spectra of P450cam wild-type, P450cam-Y96F, P450BMP, iNOSox, and nNOSox. All samples were freeze-quenched after 8 ms reaction with peroxyacetic acid. Experimental parameters: microwave power, 2.5 μW; modulation amplitude, 0.4 mT; modulation frequency, 10 kHz [9,25–28]. The thin trace labelled 'P450BMP residual' shows the residual EPR signal after subtraction of a simulated tyrosyl radical spectrum from the P450BMP spectrum. The residual signal amounts to ~30% of the total signal intensity of P450BMP and shows only a very small g-anisotropy, with an isotropic value (2.0027) consistent with a tryptophan radical (see text and [26]).

[35,36]. From the simulation of the 94-GHz EPR spectrum of the P450cam wild-type protein (Fig. 4), an isotropic hyperfine value, $A_{iso}(H_{\beta 1}) = 1.1 \pm 0.1$ mT, was obtained for one of the β-CH_2 protons [28]. Using this value in Eq. 1 with $\rho^{\pi}_{C1} = 0.38$ [36], $B' = 0$ and $B'' = 5.0$ mT [28,30], a dihedral angle of $\theta_1 = 40.5° \pm 3°$ was calculated, which matches very well the 41° obtained for Y96 from the crystal structure of substrate-free P450cam (1PHC.PDB) (Fig. 5). In order to prove this spectroscopic assignment and to investigate whether amino acid radicals may be generated on other residues, we investigated mutant Y96F, with a phenylalanine at residue 96. Indeed, mutant Y96F showed also a strong radical signal (Fig. 2). However, the EPR signature of this radical signal (Fig. 4) was changed, and revealed a significantly larger hyperfine coupling of the side-chain proton ($A_{iso}(H_{\beta 1}) = 1.55 \pm 0.05$ mT). The deduced dihedral angle θ_1 for the β-proton was in the range 23°–27°, which was consistent with the angle of 26° for Y75, seen in the crystal structure of the enzyme (Fig. 2). Furthermore, we replaced both tyrosines Y96 and Y75 by phenylalanines in an attempt to detect the proposed porphyrin radical. However, even in this Y96F–Y75F double mutant a porphyrin radical signal was not detected, but also no further radical of an amino acid side-chain was seen [28]. Neither in the wild-type nor in the mutants of P450cam did we find any indication for the supposed porphyrin-π-cation radical on a time scale equal to or longer than 8 ms after the reaction.

The iron(IV) state in the P450cam intermediate detected by Mössbauer spectroscopy

We used Mössbauer spectroscopy to see whether at least the supposed iron(IV) was formed in our experiments. Indeed, the Mössbauer spectrum of the freeze-quenched sample (Fig. 6) represented a spectral mixture of a signal of an intermediate species and the spectral pattern of the iron(III)–P450cam starting material [9,25,37]. The intermediate showed a doublet with an isomer shift of $\delta = 0.13$ mm s^{-1}, which is similar to the value observed for CPO ($\delta = 0.14$ mm s^{-1}). It is typical for iron(IV) [38]. The finding that the quadrupole splitting of P450cam (ΔE_Q=1.94 mm s^{-1}) is significantly larger than that of CPO ($\Delta E_Q = 1.02$ mm s^{-1}) might indicate differences in the local symmetry around the heme. In fact, recent quantum chemical calculations based on the density functional theory for this intermediate suggest the existence of a protonated cysteine [39].

The life time of the intermediate in P450cam

We have determined the fractions of radical and iron(IV) that were formed at different reaction times

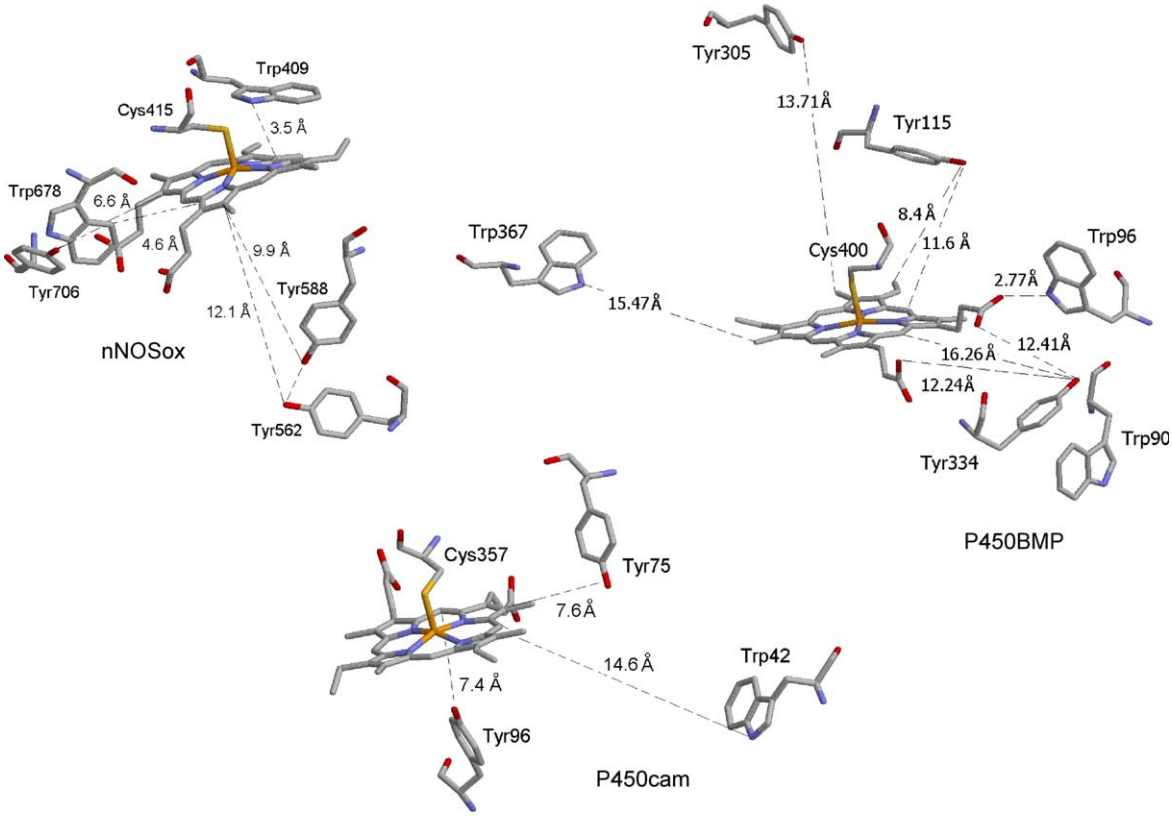

Fig. 5. Active center structure with tyrosines and tryptophans close to the heme of P450cam (1PHC.PDB), P450BMP (1FAG.PDB), and nNOSox (1OM4.PDB). The structure for iNOSox is very similar to nNOSox.

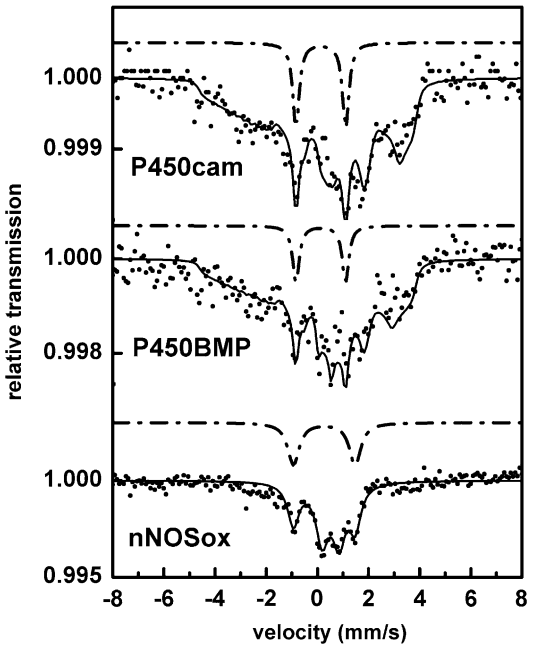

Fig. 6. Mössbauer spectra of P450cam, P450BMP, and nNOSox after reaction with PA for 8 ms [9,25–27,37] taken at 4.2 K in a field of 20 mT perpendicular to the γ-beam. The lower solid line following the experimental spectrum (points) for P450cam is a simulation using the sum of two components: an Fe(IV) species with $\delta = 0.13\ \text{mm s}^{-1}$ and $\Delta E_Q = 1.94\ \text{mm s}^{-1}$ (dashed-dotted line: $13 \pm 2\%$ relative contribution) and the Fe(III) start material ($87 \pm 2\%$ relative contribution) with the parameters given in [9]. The solid line following the experimental spectrum (points) for P450BMP is a simulation using the sum of three components: an Fe(IV) species with parameters identical to those for P450cam (dashed-dotted line: $12 \pm 3\%$ relative contribution), a minor Fe(III) species with $\delta = 0.30 \pm 0.03\ \text{mm s}^{-1}$ and $\Delta E_Q = 0.50 \pm 0.03\ \text{mm s}^{-1}$ ($7 \pm 2\%$ relative contribution) and the Fe(III) start material ($81 \pm 5\%$ relative contribution) with the parameters given in [26]. The solid line following the experimental spectrum (points) for nNOSox is a sum of two components: a doublet with $\delta = 0.27 \pm 0.03\ \text{mm s}^{-1}$ and $\Delta E_Q = 2.41 \pm 0.03\ \text{mm s}^{-1}$ (dashed-dotted line: $40 \pm 5\%$ relative contribution) and a non-heme high-spin Fe(III) impurity with $\delta = 0.52\ \text{mm s}^{-1}$ and $\Delta E_Q = 0.66\ \text{mm s}^{-1}$ ($60 \pm 5\%$ relative contribution) which is also present in the start nNOSox sample and is not effected by the PA treatment [27].

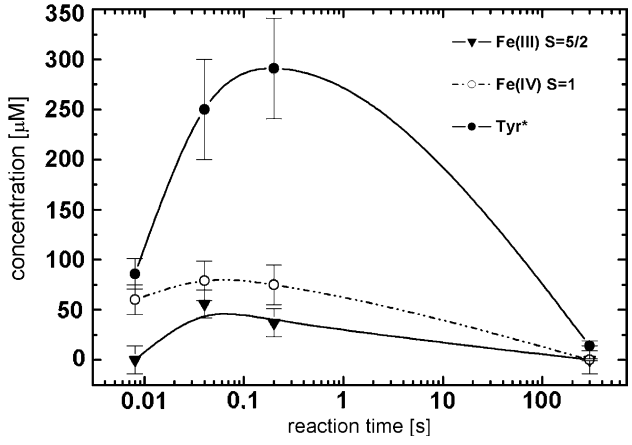

Fig. 7. Time dependence of Tyr96 radical formation (as determined from EPR) and formation of Fe(IV) and 5-coordinated ferric heme (as determined from Mössbauer spectroscopy) [37].

(Fig. 7). At 8 ms the amount of the tyrosine radical scales approximately with the amount of Fe(IV) observed. This correlation is already lost after 40 ms. The detailed analysis of the 9.6-GHz EPR spectra revealed the formation of an additional axial ferric high-spin intermediate that is increasingly formed during the time course [37]. From the concentrations shown in Fig. 7 a correlation between the amount of radical and the sum of the amounts of ferryl and ferric species seems likely. After a reaction time of 5 min only traces of the intermediate have been detected and the amount of recovered ferric starting material almost resembles (error 15–20%) that of the starting concentration. At longer reaction times bleaching of the porphyrin UV–visible absorption due to oxidative ring cleavage as a side reaction was observed [25]. A bleaching rate constant of $\sim 0.027\ \text{s}^{-1}$ has been determined at room temperature for a PA to P450 ratio of 5:1 for the substrate-free protein, which corresponds to the ratio used in the rapid-mixing/freeze-quench experiment. These experiments were, however, performed with lower absolute protein and oxidant concentrations because UV–visible spectra were recorded for detection. After 5 min this process causes a loss of heme of approximately 10–15% of the total P450 concentration, which is in the range of the accuracy for determination of the absolute concentrations from EPR data. For the shorter reaction times (<200 ms), the contribution of the bleaching process is negligibly small (<0.1%). It is notable that camphor binding in the heme pocket significantly stabilizes the protein against bleaching, indicating that oxidant binding to the heme iron is the precursor step [25]. Thus, the time course shown in Fig. 7 is consistent with the existence of a real intermediate.

Substrate hydroxylation by P450cam via the shunt pathway

As mentioned above, earlier studies on different cytochromes P450 and peracids indicated substrate conversion via the shunt pathway. This was confirmed by our studies with PA and wild-type P450cam [25]. The product 5-exo-hydroxy-camphor was detected by gas chromatography–mass spectrometry analysis from samples obtained in separate activity experiments for a PA- to P450cam ratio of 38:1 and a long reaction time of 130 min, because the hydroxylation yield was very low. It turned out that the reason for the low yield was that the substrate camphor bound near the heme hindered the access of peracid to the heme pocket. This was concluded from the finding that camphor binding strongly inhibited tyrosine radical formation (0.4%) compared to that on the substrate-free protein (15%). However, the fraction of tyrosine radical formed was again increased when substrates with a higher mobility (i.e., norcamphor (1.2%) or norbornane (1.6–2%)) were bound in the heme pocket, which allowed better heme pocket accessibility (rigidity factors: 1R-camphor (6.81), norcamphor (1.75), and norbornane (1.86), expressed as inverse values of the loss of high-spin state content within 10 min per degree temperature determined

in negative-temperature jump experiments (K/([% high-spin loss] [10 min])) [40,41].

The iron-oxo intermediate in cytochrome P450 BMP (CYP102)

The different studies on P450cam described above suggest that in the initial step peroxyacetic acid binds to the heme iron and might form the iron(IV)–porphyrin-π-cation radical. However, the porphyrin radical is quickly quenched by subsequent intramolecular electron transfer from the tyrosine (Fig. 3). This makes it impossible to detect the porphyrin radical itself. To check whether this phenomenon is specific for P450cam we performed analogous studies on cytochrome P450BM3 from *Bacillus megaterium* (CYP102) [26], which hydroxylates fatty acids. P450BM3 expresses as a fusion protein with its reductase, a flavin protein [42,43]. To avoid interference in the EPR spectra caused by possible radical formation of the flavin when reacting with peracid, we used only the heme domain of P450BM3 (P450BMP) in our studies.

The findings on substrate-free P450BMP agree with the observations on P450cam. The 9.6-GHz EPR spectrum of P450BMP, which reacted with PA within 8 ms, showed an unresolved narrow intense radical signal with $g \sim 2$, which accounts for $19 \pm 5\%$ of the total observable EPR intensity (Fig. 2). The remaining spectral signals ($81 \pm 5\%$) originate from the starting material with g-values of 2.42, 2.25, and 1.91. After ca. 3 min reaction time the spectral pattern of the radical has disappeared and the EPR signals of the start material are recovered.

All three components of the g-tensor (g_x, g_y, and g_z) of the radical signal in P450BMP were again resolved at the 10-fold higher magnetic field in the 94-GHz EPR spectrum (Fig. 4). The spectrum of P450BMP had an overall shape similar to that of wild-type P450cam. However, compared to the P450cam spectrum (Fig. 4), the strong negative signal component on the high-field side (at 3355 mT) was by far too intense for a g_z-component of a tyrosine radical alone. The simulation of the EPR spectrum of P450BMP yielded the g-values: $g_z = 2.0022(1)$, $g_y = 2.0043(1)$, and a range of g_x-values between 2.0070 and 2.0082 (numbers in brackets are errors in the last digit). Furthermore, an upper limit for the isotropic part ($A_{iso} = (A_x + A_y + A_z)/3$) of the β-proton hf-tensor of 0.7–1.1 mT was obtained, depending whether one or two of these protons contribute. Inspection of the X-ray structure of P450BMP (1FAG.PDB) (Fig. 5) shows that of the tyrosines in the neighborhood of the heme, Tyr305 and Tyr334 both have side-chain orientations, consistent with the observed small β-proton hf tensors, whereas from the side-chain orientation of Tyr115 a large A_{iso} value (1.8–2.0 mT) is expected for one β-proton, which is beyond the experimental value. While the low-field side and the g_y-component of the experimental spectrum were fairly well represented in the 94-GHz EPR simulations, there was obviously a strong, almost symmetrical line in the P450BMP residual spectrum on the high-field side (Fig. 4), which amounted to 30% of the total signal intensity [26]. Interestingly, the zero crossing of this residual spectrum (Fig. 4) corresponded to $g = 2.0027(2)$, which fits well with the isotropic part ($g_{iso} = (g_x + g_y + g_z)/3$) of the g-tensor reported for tryptophan radicals [30]. All three tryptophans in the neighborhood of the heme (Trp90, Trp96, Trp367) have side-chain orientations leading to hf tensors for the β-protons, which would be consistent with the spectral width of this residual signal.

The Mössbauer spectrum obtained from the freeze-quenched P450BMP sample after reaction with PA for 8 ms reveals, besides a minor Fe(III) species with $\delta = 0.30\ \text{mm s}^{-1}$ and $\Delta E_Q = 0.50\ \text{mm s}^{-1}$ ($7 \pm 2\%$ relative contribution) and the spectrum of the ferric starting material ($81 \pm 5\%$ relative contribution), the formation of a Fe(IV) species with $\delta = 0.13\ \text{mm s}^{-1}$ and $\Delta E_Q = 1.94\ \text{mm s}^{-1}$ ($12 \pm 3\%$ relative contribution) (Fig. 6). The last species has also been observed in P450cam, indicating that the heme iron exists as a transient Fe(IV) species in both P450cam and P450BMP.

The iron-oxo intermediate in nitric oxide synthases

Nitric oxide synthases (NOS) catalyze the transformation of L-arginine to citrulline and NO [44] and belong, like P450, to the thiolate heme proteins because of the negatively charged sulfur of the cysteine as proximal heme iron ligand. Similarly, to P450BM3, it expresses as a fusion protein with its reductase. The latter can easily be cleaved off releasing the oxygenase domain (heme domain; NOSox). For the same reason as discussed for P450BM3, only the oxygenase domain (expressed in *Escherichia coli*) has been studied [27]. From the three known isoenzymes [44] we have studied the inducible NOS (iNOSox) from the mouse and the neuronal NOS (nNOSox) from the rat [27].

The 9.6-GHz EPR spectrum of nNOSox, which reacted with PA within 8 ms, was dominated by a strong radical signal, which accounts for $80 \pm 5\%$ of the total observable EPR intensity (Fig. 2). In contrast to the observations on P450, the spectrum did not show any signal originating from the starting material. Instead, an almost axial signal with g-values of 2.24, 2.23, and 1.96 ($20 \pm 5\%$ relative spin concentration) representing an $S = 1/2$ system of unknown origin was observed. For the case of iNOSox the same signals were observed, except with a lower radical yield ($11 \pm 5\%$) and a higher contribution of the unknown $S = 1/2$ system ($89 \pm 5\%$) (Fig. 2). There was no significant change in the spectrum for longer times up to 200 ms. However, after ca. 3 min reaction time the spectral pattern of the radical and the unknown species disappeared and the EPR signals of the start material were recovered.

The radical signal has also been studied in more detail by high-frequency EPR. In the 94-GHz EPR spectrum of substrate-free nNOSox all three g-values were clearly sepa-

rated in the spectrum and only g_z showed indications of hyperfine structure (Fig. 4). The simulation of the spectrum yielded g-values of $g_z = 2.00215 \pm 0.00005$ and $g_y = 2.0043 \pm 0.0001$. The g_x-component was broadened, as observed for P450, and was simulated using a distribution of g_x-values between 2.0065 and 2.0070 [27]. There was no hyperfine structure observed in the 94-GHz EPR spectrum except for a weak indication on the g_z-component. However, the 9.6-GHz EPR spectrum showed a hyperfine structure at elevated temperature, from which the hyperfine values of two side-chain protons were obtained ($A_{iso}(H_{\beta 1}) = 0.57 \pm 0.1$ mT, $A_{iso}(H_{\beta 2}) = 0.50 \pm 0.1$ mT) [27]. From these hyperfine values, using Eq. 1, dihedral angles of $\theta_1 = 58° \pm 4°$ and $\theta_2 = 60° \pm 4°$ were obtained. These values agree well with those obtained for Tyr562 from the crystal structure of nNOSox (1OM4.PDB) (Fig. 5) ($\theta_1 = 58°$ and $\theta_2 = 62°$). The simulation of the 94-GHz EPR spectrum of nNOSox (Fig. 4) was improved when a superposition with a further tyrosine radical (about 25% of the relative area) was assumed, which had a large hyperfine coupling of only one side-chain proton with $A_{iso}(H_{\beta})$ of approximately 1.4–1.6 mT. Such hyperfine couplings are expected from the two other tyrosines close to the heme, Tyr588 and/or Tyr706, based on their side-chain geometry. Tyr706 is the tyrosine closest to the heme edge (Fig. 5), but probably does not contribute to the spectrum. The Tyr706Phe mutant showed a 94-GHz spectrum, which is identical to that of the wild-type protein [27]. The almost identical signals in the 94-GHz spectrum of the radical intermediate of the structurally very similar iNOSox and nNOSox (Fig. 4) leads to the conclusion that the analogue Tyr341 is the major radical site in iNOSox (1NOD.PDB), while Tyr362 may be a minor contributor.

The origin of the transient iron-centered nearly axial $S = 1/2$ signal with g-values of 2.24, 2.23, and 1.96 is not identified so far. An Fe(IV)=O porphyrin-π-cation radical with the Fe(IV) being in the $S = 1$ spin state, which is strongly antiferromagnetically exchange-coupled to the radical spin $S' = 1/2$ delocalized on the heme ring, has been discussed [27]. The presence of a radical on the cysteine ligand might also be taken into account. The concentration of this species (~43 μM in our experiments) is probably too low to be detectable by Mössbauer spectroscopy. Indeed, the Mössbauer spectrum for nNOSox (Fig. 6) does not indicate an Fe(IV) state which typically has isomer shifts of <0.15 mm s^{-1}. Instead, the doublet of the intermediate shows parameters of $\delta = 0.27$ mm s^{-1} and $\Delta E_Q = 2.41$ mm s^{-1} which resemble more those of a Fe(II)—O_2 moiety. The formation of a transient dioxygen complex is unlikely because PA acts usually as an oxidant and not as a reductant. Another possibility, compatible with the Mössbauer parameters, is the presence of a ferric low-spin species which magnetically couples to an amino acid radical. Trp409 in nNOSox has been proposed for such a radical site [27] because it is only 3.5 Å away from the closest heme edge (Fig. 5).

Amino acid radical formation as general phenomenon in heme protein iron-oxo intermediates

In summary, the results of the rapid-mixing/freeze-quench experiments on P450cam, P450BMP, NOS, and CPO [9,25–28,37,45] show that a similar proximal ligand (negatively charged sulfur of a cysteine) does not necessarily mean that the Compound I intermediate and its first reaction products are identical in these systems, as was hitherto assumed. The observation of the formation of tyrosine and tryptophan radicals in the iron-oxo species leads to the conclusion that intramolecular electron transfer from the protein residues to the heme occurs if a porphyrin radical is initially produced in the reaction with the oxidant (Fig. 3). Interestingly, radicals have been observed by EPR already in a few cases for P450 other than P450cam, both during reaction with oxidants and during turnover [46–48]. Indeed, even for CPO, a small-radical EPR signal, not assigned so far, after reaction times of around 200 ms has been detected [14,25].

While cpd I in cytochrome *c* peroxidase with its Fe(IV)=O tryptophan radical system [49,50] was regarded as an exception for many years, there are now well-established examples where a radical on the protein, in particular a tyrosine radical, has been observed. Miller et al. [51] found for the Phe172Tyr mutant of horseradish peroxidase in the reaction with H_2O_2 that ~10% of the mutant carries a protein radical, presumably at Tyr172. Ivancich et al. [31,34,52,53] observed by EPR a tyrosine radical when bovine liver catalase reacts with PA. This radical is directly formed by electron transfer to the porphyrin-π-cation radical. Recently the same group reported the formation of a tyrosine radical after treatment of turnip peroxidase isozymes with hydrogen peroxide at pH 7.7, accompanied by the formation of a ferryl iron-oxo porphyrin π-cation radical system [33]. Tyrosine radicals have also been found earlier in prostaglandin *H* synthase [54] and cytochrome *c* oxidase [55]. Tyrosine 167 in cytochrome *c* oxidase from *Paracoccus denitrificans* has recently been assigned as the origin of the radical when the enzyme reacts with hydrogen peroxide [56]. Even for cytochrome *c* peroxidase the oxidation of tyrosine is favored over tryptophan oxidation when the tryptophan nearest to the heme is removed or its interaction with the environment (Asp235) is perturbed [57]. Tryptophan radicals have been observed also in lignin-type versatile peroxidases [58]. This list of examples is far from being complete and it may be expected that future studies on reaction intermediates will reveal the existence or co-existence of yet undetected radicals, such as those located at the cysteine proximal ligand in thiolate heme proteins, as suggested by recent X-ray absorption spectroscopy investigations of CPO [17]. This has also been discussed as possible species in P450 cpd I intermediates [59–61].

In many cases this radical formation might function as an important side reaction which competes with the main reaction of these enzymes (analogous to the uncoupling side reaction for H_2O_2 formation (Fig. 1)) [41,45]. In other cases,

as reported for certain peroxidases [58,62], these amino acid radicals might be even involved in the catalytic cycle.

Acknowledgments

We are very grateful to Alfred X. Trautwein (University of Lübeck) for his help in initiating these studies and for his continuous support. Instrumental high-field EPR support from Robert Bittl (Free University Berlin) is gratefully acknowleged. These studies were funded by the Deutsche Forschungsgemeinschaft, Grants Ju229/4-(1-3), Ju229/5-1, Sk35/3-(3-5) to C.J.; Le 812/2-1 to F.L.; Tr97/26-(1-3) to AXT; and Schu1251/3-1 to V.S.

References

[1] O. Hayaishi, M. Katagiri, S. Rothberg, Mechanism of the pyrocatechase reaction, J. Am. Chem. Soc. 77 (1955) 5450.
[2] R.W. Estabrook, A passion for P450s (Remembrance of the early history of research on cytochrome P450), Drug Metab. Dispos. 31 (2003) 1461–1473.
[3] M. Klingenberg, Pigments of rat liver microsomes, Arch. Biochem. Biophys. 75 (1958) 376–386.
[4] D. Garfinkel, Studies on pig liver microsomes. I. Enzymic and pigment composition of different microsomal fractions, Arch. Biochem. Biophys. 77 (1958) 493–509.
[5] T. Omura, R. Sato, A new cytochrome in liver microsomes, J. Biol. Chem. 237 (1964) PC1375–PC1376.
[6] T. Omura, R. Sato, The carbon monoxide-binding pigment of liver microsomes. I. Evidence for hemeprotein nature, J. Biol. Chem. 239 (1964) 2370–2378.
[7] J.T. Groves, Models and mechanisms of cytochrome P450 action, in: P.R. Ortiz de Montellano (Ed.), Cytochrome P450, Structure, Mechanism, and Biochemistry, Kluwer Academic/Plenum, New York, 2005, pp. 1–43.
[8] H. Fujii, Electronic structure and reactivity of high-valent oxo iron porphyrins, Coord. Chem. Rev. 226 (2002) 51–60.
[9] V. Schünemann, C. Jung, A.X. Trautwein, D. Mandon, R. Weiss, Intermediates in the reaction of substrate-free cytochrome P450cam with peroxy acetic acid, FEBS Lett. 479 (2000) 149–154.
[10] P.R. Ortiz deMontellano, Cytochrome P450: Structure, Mechanism, and Biochemistry, third ed., Kluwer Academic/Plenum, New York, 2005.
[11] V. Ullrich, H.J. Staudinger, Model systems in studies of the chemistry and the enzymatic activation of oxygen, in: B.B. Brodie, J.R. Gillette, H.S. Ackermann (Eds.), Handbuch der Experimentellen Pharmakologie, Vol. 28/2, Springer-Verlag, Berlin, New york, 1971, pp. 251–263.
[12] M.M. Palcic, R. Rutter, T. Araiso, L.P. Hager, H.B. Dunford, Spectrum of chloroperoxidase compound I, Biochem. Biophys. Res. Commun. 94 (1980) 1123–1127.
[13] T. Egawa, D.A. Proshlyakov, H. Miki, R. Makino, T. Ogura, T. Kitagawa, Y. Ishimura, Effects of a thiolate axial ligand on the π–π^* electronic states of oxoferryl porphyrins: a study of the optical and resonance Raman spectra of compound I and II of chloroperoxidase, J. Biol. Inorg. Chem. 6 (2001) 46–54.
[14] R. Rutter, L.P. Hager, H. Dhonau, M. Hendrich, M. Valentine, P. Debrunner, Chloroperoxidase compound I: electron paramagnetic resonance and Mössbauer studies, Biochemistry 23 (1984) 6809–6816.
[15] T. Egawa, H. Miki, T. Ogura, R. Makino, Y. Ishimura, T. Kitagawa, Observation of the Fe^{IV}=O stretching Raman band for a thiolate-ligated heme protein Compound I of chloroperoxidase, FEBS Lett. 305 (1992) 206–208.
[16] K. Nakamoto, Resonance Raman spectra and biological significance of high-valent iron(IV,V) porphyrins, Coord. Chem. Rev. 226 (2002) 153–165.
[17] M.T. Green, J.H. Dawson, H.B. Gray, Oxoiron(IV) in chloroperoxidase compound II is basic: implication for P450 chemistry, Science 304 (2004) 1653–1656.
[18] T. Egawa, H. Shimada, Y. Ishimura, Evidence for Compound I formation in the reaction of cytochrome P450cam with *m*-chloroperbenzoic acid, Biochem. Biophys. Res. Commun. 201 (1994) 1464–1469.
[19] D.G. Kellner, S.-C. Hung, K.E. Weiss, S.G. Sligar, Kinetic characterization of compound I formation in the thermostable cytochrome P450 CYP119, J. Biol. Chem. 277 (2002) 9641–9644.
[20] T.C. Pederson, R.H. Austin, I.C. Gunsalus, Redox and ligand dynamics in $P450_{cam}$–putidaredoxin complexes, in: V. Ullrich, I. Roots, A. Hildebrandt, R.W. Estabrook (Eds.), Microsomes and Drug Oxidations, Pergamon, Oxford, 1977, pp. 275–283.
[21] G.C. Wagner, M.M. Palcic, H.B. Dunford, Absorption spectra of cytochrome P450cam in the reaction with peroxy acids, FEBS Lett. 156 (1983) 244–248.
[22] S.G. Sligar, B.S. Shastry, I.C. Gunsalus, Oxygen reactions of the P450 heme protein, in: V. Ullrich, I. Roots, A. Hildebrandt, R.W. Estabrook (Eds.), Microsomes and Drug Oxidations, Pergamon, Oxford, 1977, pp. 202–209.
[23] S. Prasad, S. Mitra, Substrate modulate compound I formation in peroxide shunt pathway of *Pseudomonas putida* cytochrome P450cam, Biochem. Biophys. Res. Commun. 314 (2004) 610–614.
[24] T. Spolitak, J.H. Dawson, D.P. Ballou, Reaction of ferric cytochrome P450cam with peracids: Kinetic characterization of intermediates on the reaction pathway, J. Biol. Chem. 280 (2005) 20300–20309.
[25] V. Schünemann, C. Jung, J. Terner, A.X. Trautwein, R. Weiss, Spectroscopic studies of peroxyacetic acid reaction intermediate of cytochrome P450cam and chloroperoxidase, J. Inorg. Biochem. 91 (2002) 586–596.
[26] C. Jung, V. Schünemann, F. Lendzian, A.X. Trautwein, J. Contzen, M. Galander, L.H. Böttger, M. Richter, A.-L. Barra, Spectroscopic characterization of the iron-oxo intermediate in cytochrome P450, Biol. Chem. (2005) (in press).
[27] C. Jung, F. Lendzian, V. Schünemann, M. Richter, L.H. Böttger, A.X. Trautwein, J. Contzen, M. Galander, D.K. Ghosh, A.-L. Barra, Multi-frequency EPR and Mössbauer spectroscopic studies on freeze-quenched reaction intermediates of nitric oxide synthase, Magn. Res. Chem. (2005) (in press).
[28] V. Schünemann, F. Lendzian, C. Jung, J. Contzen, A.-L. Barra, S.G. Sligar, A.X. Trautwein, Tyrosine radical formation in the reaction of wild type and mutant cytochrome P450cam with peroxy acids: a multifrequency EPR study of intermediates on the millisecond time scale, J. Biol. Chem. 279 (2004) 10919–10930.
[29] G.C. Wagner, I.C. Gunsalus, Cytochrome P450: Structure and states, in: H.B. Dunford (Ed.), The Biological Chemistry of Iron, Reidel, Dordrecht, 1982, pp. 405–412.
[30] G. Bleifuß, M. Kolberg, S. Pötsch, W. Hofbauer, R. Bittl, L. Lubitz, A. Gräslung, G. Lassmann, F. Lendzian, Tryptophan and tyrosyl radicals in ribonucleotide reductase: a comparative high-field EPR study at 94-GHz, Biochemistry 40 (2001) 15362–15368.
[31] A. Ivancich, C. Jakopitsch, M. Auer, S. Un, C. Obinger, Protein-based radicals in the catalase-peroxidase of synechocystis PCC6803: a multifrequency EPR investigation of wild-type and variants on the environment of the heme active site, J. Am. Chem. Soc. 125 (2003) 14093–14102.
[32] F. Lendzian, Structure and interactions of amino acid radicals in class I ribonucleotide reductase studied by ENDOR and high-field EPR spectroscopy, Biochim. Biophys. Acta 1707 (2005) 67–90.
[33] A. Ivancich, G. Mazza, A. Desbois, Comparative electron paramagnetic resonance study of radical intermediates in turnip peroxidase isozymes, Biochemistry 40 (2001) 6860–6866.
[34] A. Ivancich, T.A. Mattioli, S. Un, Effect of protein microenvironment on tyrosyl radicals. A high-field (285-GHz) EPR, resonance Raman, and hybrid density functional study, J. Am. Chem. Soc. 121 (1999) 5743–5753.

[35] C.W. Hoganson, M. Sahlin, B.-M. Sjöberg, G.T. Babcock, Electron magnetic resonance of the tyrosyl radical in ribonucleotide reductase from *Escherichia coli*, J. Am. Chem. Soc. 118 (1996) 4672–4679.
[36] F. Himo, A. Gräslund, L.A. Eriksson, Density functional calculations on model tyrosyl radicals, Biophys. J. 72 (1997) 1556–1567.
[37] V. Schünemann, C. Jung, F. Lendzian, A.-L. Barra, Th. Teschner, A.X. Trautwein, Mössbauer- and EPR-snapshots of an enzymatic reaction: the cytochrome P450 reaction cycle, Hyperfine Interact. 156/157 (2004) 247–256.
[38] A.X. Trautwein, E. Bill, E.L. Bominaar, H. Winkler, Iron-containing proteins and related analogs—complementary Mössbauer, EPR and magnetic susceptibility studies, Struct. Bond. 78 (1991) 1–95.
[39] Y. Zhang, E. Oldfield, Cytochrome P450: an investigation of the Mössbauer spectra of a reaction intermediate and an Fe(IV)=O model system, J. Am. Chem. Soc. 126 (2004) 4470–4471.
[40] H. Schulze, G. Hui Bon Hoa, C. Jung, Mobility of norbornane-type substrates and water accessibility in cytochrome P-450cam, Biochim. Biophys. Acta 1338 (1997) 77–92.
[41] C. Jung, S.A. Kozin, B. Canny, J.-C. Chervin, G. Hui Bon Hoa, Compressibility and uncoupling of cytochrome P450cam: high pressure FTIR and activity studies, Biochem. Biophys. Res. Commun. 312 (2003) 197–203.
[42] I.F. Sevrioukova, G. Truan, J.A. Peterson, The flavoprotein domain of P450BM-3: expression, purification, and properties of the flavin adenine dinucleotide- and flavin mononucleotide-binding subdomains, Biochemistry 35 (1996) 7528–7535.
[43] I.F. Sevrioukova, G. Truan, J.A. Peterson, Reconstitution of the fatty acid hydroxylase activity of cytochrome P450BM-3 utilizing its functional domains, Arch. Biochem. Biophys. 340 (1997) 231–238.
[44] K. Alderton, C.E. Cooper, R.G. Knowles, Nitric oxide synthases: structure, function and inhibition, Biochem. J. 357 (2001) 593–615.
[45] C. Jung, F. Lendzian, V. Schünemann, A.X. Trautwein, J. Contzen, M. Richter, M. Galander, D.K. Ghosh, S.A. Kozin, Uncoupling of the P450 reaction cycle related to protein structural properties, in: F. Oesch (Ed.), Proceedings of the 15th International Symposium on Microsomes and Drug Oxidations, Mainz, Germany, July 4–9, Monduzzi Editore—International Proceedings Division, Bologna, 2004, pp. 87–91.
[46] J. Capdevila, R.W. Estabrook, R.A. Prough, Differences in the mechanism of NADPH- and cumene hydroperoxide-supported reactions of cytochrome P-450, Arch. Biochem. Biophys. 200 (1980) 186–195.
[47] P.R. Ortiz de Montellano, K.L. Kunze, H.S. Beilan, C. Wheeler, Destruction of cytochrome P-450 by vinyl fluoride, fluroxene, and acetyl. Evidence for a radical intermediate in olefin oxidation, Biochemistry 21 (1982) 1331–1339.
[48] C. Larroque, R. Lange, L. Maurin, A. Bienvenue, J.E. van Lier, On the nature of the cytochrome P450scc "ultimative oxidant": characterization of a productive radical intermediate, Arch. Biochem. Biophys. 282 (1990) 198–201.
[49] M. Sivaraja, D.B. Goodin, M. Smith, B.M. Hoffman, Identification by ENDOR of Trp191 as the free-radical site in cytochrome *c* peroxidase compound ES, Science 245 (1989) 738–740.
[50] T.P. Barrows, B. Bhaskar, T.L. Poulos, Electrostatic control of the tryptophan radical in cytochrome *c* peroxidase, Biochemistry 43 (2004) 8826–8834.
[51] V.P. Miller, D.B. Goodin, A.E. Friedman, C. Hartman, P.R. Ortiz de Montellano, Horseradish peroxidase Phe → Tyr mutant, J. Biol. Chem. 270 (1995) 18413–18419.
[52] A. Ivancich, H.M. Joue, J. Gaillard, EPR evidence for a tyrosyl radical intermediate in bovine liver catalase, J. Am. Chem. Soc. 118 (1996) 12852–12853.
[53] A. Ivancich, H.M. Joue, B. Sartor, J. Gaillard, EPR investigation of compound I in *Proteus mirabilis* and bovine liver catalases: formation of porphyrin and tyrosyl radical intermediates, Biochemistry 36 (1997) 9356–9364.
[54] R. Karthein, R. Dietz, W. Nastainzyk, H.H. Ruf, Higher oxidation states of prostaglandin *H* synthase. EPR study of a transient tyrosyl radical in the enzyme during the peroxidase reaction, Eur. J. Biochem. 171 (1988) 313–320.
[55] G. Lang, K. Spartalian, T. Yonetani, Mossbauer spectroscopic study of compound ES of cytochrome *c* peroxidase, Biochim. Biophys. Acta 451 (1976) 250–258.
[56] K. Budiman, A. Kannt, S. Lyubenova, O.M.H. Richter, B. Ludwig, H. Michel, F. MacMillan, Tyrosine 167: the origin of the radical species observed in the reaction of cytochrome *c* oxidase with hydrogen peroxide in *Paracoccus denitrificans*, Biochemistry 43 (2004) 11709–11716.
[57] L.A. Fishel, M.F. Farnum, J.M. Mauro, M.A. Miller, J. Kraut, Compound I radical in site-directed mutants of cytochrome *c* peroxidase as probed by electron paramagnetic resonance and electron-nuclear double resonance, Biochemistry 30 (1991) 1986–1996.
[58] R. Pogni, M.C. Baratto, S. Giansanti, C. Teutloff, J. Verdin, B. Valderrama, F. Lendzian, W. Lubitz, R. Vazquez-Duhalt, R. Basosi, Tryptophan-based radical in the catalytic mechanism of versatile peroxidase from *Bjerkandera adusta*, Biochemistry 44 (2005) 4267–4274.
[59] M.T. Green, Evidence for sulfur-based radicals in thiolate compound I intermediates, J. Am. Chem. Soc. 121 (1999) 7939–7940.
[60] V. Ullrich, Thoughts on thiolate tethering. Tribute and thanks to a teacher, Arch. Biochem. Biophys. 409 (2003) 45–51.
[61] S. Shaik, S.P. De Visser, Computational approaches to cytochrome P450 function, in: P.R. Ortiz de Montellano (Ed.), Cytochrome P450, Structure, Mechanism, and Biochemistry, Kluwer Academic/Plenum, New York, 2005, pp. 45–85.
[62] W. Blodig, A.T. Smith, W.A. Doyle, K.J. Piontek, Crystal structures of pristine and oxidatively processed lignin peroxidase expressed in *Escherichia coli* and of the W171F variant that eliminates the redox active tryptophan 171: Implications for the reaction mechanism, Mol. Biol. 305 (2001) 851–861.
[63] A. Mezzetti, A.L. Maniero, M. Brustolon, G. Giacometti, L.C. Brunel, A tyrosyl radical in an irradiated single crystal of *N*-acetyl-L-tyrosine studied by X-band cw-EPR, high-frequency EPR, and ENDOR spectroscopies, J. Phys. Chem. A 103 (1999) 9636–9643.